Available online at www.sciencedirect.com
ScienceDirect
Journal of Sound and Vibration 305 (2007) 357–361
JOURNAL OF SOUND AND VIBRATION
www.elsevier.com/locate/jsvi

Discussion

Discussions on "composite element method for vibration analysis of structure"

Z.R. Lu[a], S.S. Law[b,*]

[a]School of Engineering, Sun Yat-sen University, Guangzhou 510275, PR China
[b]Civil and Structural Engineering Department, The Hong Kong Polytechnic University, Hunghom, Kowloon, Hong Kong, China

Received 10 March 2006; received in revised form 25 April 2007; accepted 29 April 2007

1. Introduction

Composite element method (CEM) was proposed by Zeng and two companion papers were published [1,2]. The solution of CEM is obtained by combining the conventional finite element method (FEM) [3] and the closed-form solutions from the classical theory [4]. The accuracy of the CEM can be improved using two approaches, namely, *h*- and *c*-version. The *h*-version means the refinement of the finite element mesh, which is the same as the FEM. The *c*-version is the increase of degrees-of-freedom (dofs) related to the classical theory. The *c*-refinement shows the super-convergence in the results. Numerical examples showed that the CEM is more accurate than the FEM with the same number of total dofs. This shows that the CEM is computationally efficient and highly accurate.

In this discussion, two ways are presented to further improve the CEM: (a) The analytical shape functions from the classical theory should observe certain special boundary conditions, and this will lead to different kinds of shape functions in the displacement field, U_{CT}. However, in Refs. [1,2], the shape functions are the same for both a bar element and a beam element. In this discussion, the shape functions in U_{CT} are different according to the different boundary conditions of the beam; and (b) In Refs. [1,2], the entries of the coupling term of the *q*-coordinate and the *c*-coordinate in the stiffness matrix should not always be null since the interpolation polynomials of the FEM and the shapes functions of the U_{CT} do not automatically satisfy the orthogonal condition. The CEM is improved with the above two modifications, and the solutions are found better than the original ones. When the structure is discretized into one-member-one element configuration, it is found that the number of natural frequency that converges to the analytical solutions is the same as the number of *c*-dof.

2. The composite element method

The displacement field of the CEM is described as the combination of the conventional polynomials of the FEM and the shape functions of the classical theory as shown below:

$$U_{CEM}(\xi) = U_{FEM}(\xi) + U_{CT}(\xi), \tag{1}$$

*Corresponding author.
E-mail address: cesslaw@polyu.edu.hk (S.S. Law).

0022-460X/$ - see front matter
doi:10.1016/j.jsv.2007.04.047

where $U_{\mathrm{FEM}}(\xi)$ and $U_{\mathrm{CT}}(\xi)$ are the two parts of the CEM displacement field. The first part is obtained from the FEM:

$$U_{\mathrm{FEM}}(\xi) = N(\xi)q, \tag{2}$$

where $N(\xi)$ is the shape function of FEM and q the nodal coordinate.

The second part is shown as

$$U_{\mathrm{CT}}(\xi) = \varphi(\xi)c, \tag{3}$$

where $\varphi(\xi)$ is the analytical function series from the classical theory and c the field coordinate.

It is obvious that the CEM can be refined using h-refinement by increasing the number of the element in the discretization. In addition, it can also be refined by c-refinement technique, i.e., increase the number of the analytical shape functions in Eq. (3). This kind of refinement has the advantage that there is no need to recalculate the whole stiffness and mass matrices except for those related to the new dofs.

The analytical shapes function used in this discussion is determined according to the different boundary conditions of the beam which is different from Refs. [1,2]. The shapes functions for different boundary conditions are given in Appendices A and B. Once the displacement field of the CEM is determined, the remaining step for obtaining the stiffness and mass matrices is similar to those with the conventional FEM, and it is not repeated here.

3. Numerical example

3.1. A free–clamped beam

The numerical example of a free–clamped beam in Ref. [2] as shown in Fig. 1 is restudied. The length of the beam is L, the mass density is ρ and the Young's modulus is E. The beam is modeled with one element only and 1c-dof, 4c-dof, 6c-dof and 10c-dof of the shape function of a beam are chosen. Let

$$\lambda_i = \frac{\rho A L^4}{EI}\omega_i^2, \tag{4}$$

where ω_i is the ith natural frequency. Tables 1–3 give the comparison of results from Ref. [2] and those from the modified CEM. The suggested improvements only affect the stiffness matrix of the composite element while the mass matrix is computed according to the original CEM. Table 1 shows the effects of the inclusion of the coupling terms in the stiffness matrix of the composite element on the natural frequencies. All the results are based on the shape functions with clamp–clamped boundary conditions. The effect on the natural frequencies is found small and the results are found close to those from the CEM. The coupling terms of the stiffness matrix of the composite element with 5c-dof shown in Appendix B are noted small and the omission of them would not cause too large error in the final results. Table 2 shows the natural frequencies using shape functions with the clamped–free boundary conditions and without the coupling terms in the stiffness matrix. The results err more from the analytical solutions than those from the CEM indicating the effect of the coupling terms of the stiffness matrix has large effect on the natural frequencies when the shape functions of

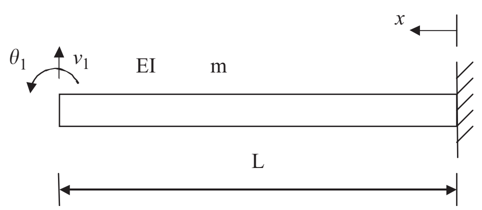

Fig. 1. A free–clamped beam.

Table 1
Effect of the coupling coordinates on the natural frequencies (Hz) (free–clamped beam)

Order	Exact	CEM ($1\times 1c$)*	CEM ($1\times 4c$)*	CEM ($1\times 6c$)*	CEM ($1\times 10c$)*
λ_1	1.875104	1.875429/1.875429	1.875109/1.875109	1.875105/1.875105	1.875104/1.875104
λ_2	4.694091		4.694419/4.694419	4.694165/ 4.694165	4.694100/4.694100
λ_3	7.854757		7.847543/7.847543	7.855485/7.855485	7.854857/7.854857
λ_4	10.99554		11.00451/11.00451	10.99836/10.99836	10.99599/10.99599
λ_5	14.13717			14.14405/14.14405	14.13846/14.13854
λ_6	17.27876			17.29133/17.29133	17.28154/17.28157
λ_7	20.42035				20.42553/20.42555
λ_8	23.56195				23.57026/23.57028
λ_9	26.70354				26.71553/26.71556
λ_{10}	29.84513				29.86089/29.86092

Note: The symbol CEM ($1\times 1c$) means using one composite element with 1-c dof; CEM ($1\times 4c$) means using one composite element with 4-c dof; $-/-$ denotes the solution of modified CEM (with coupling term only) and CEM, respectively.

Table 2
Effect of the boundary conditions on the natural frequency (Hz) (free–clamped beam)

Order	Exact	CEM ($1\times 1c$)*	CEM ($1\times 4c$)*	CEM ($1\times 6c$)*	CEM ($1\times 10c$)*
λ_1	1.875104	1.578648/1.875429	1.578644/1.875109	1.578642/1.875105	1.578642/1.875104
λ_2	4.694091		4.326955/4.694419	4.326847/ 4.694165	4.326823/4.694100
λ_3	7.854757		7.630953/7.847543	7.630397/7.855485	7.630192/7.854857
λ_4	10.99554		10.92315/11.00451	10.91921/10.99836	10.91816/10.99599
λ_5	14.13717			14.09228/14.14405	14.08909/14.13854
λ_6	17.27876			17.26013/17.29133	17.25150/17.28157
λ_7	20.42035				20.40862/20.42555
λ_8	23.56195				23.56287/23.57028
λ_9	26.70354				26.716339/26.71556
λ_{10}	29.84513				29.87301/29.86092

Note: $-/-$ denotes the solution of modified CEM (with shape functions only) and CEM, respectively.

Table 3
Comparison on the natural frequencies (Hz) (free–clamped beam)

Order	Exact	CEM ($1\times 1c$)*	CEM ($1\times 4c$)*	CEM ($1\times 6c$)*	CEM ($1\times 10c$)*
λ_1	1.875104	1.875104/1.875429	1.875104/1.875109	1.875104/1.875105	1.875104/1.875104
λ_2	4.694091		4.694091/4.694419	4.694091/4.694165	4.694091/4.694100
λ_3	7.854757		7.854757/7.847543	7.854757/7.855485	7.854757/7.854857
λ_4	10.99554		10.99554/11.00451	10.99554/10.99836	10.99554/10.99599
λ_5	14.13717			14.13717/14.14405	14.13717/14.13854
λ_6	17.27876			17.27876/17.29133	17.27876/17.28157
λ_7	20.42035				20.42037/20.42555
λ_8	23.56195				23.56197/23.57028
λ_9	26.70354				26.70357/26.71556
λ_{10}	29.84513				29.84515/29.86092

Note: $-/-$ denotes the solution of modified CEM (with shape functions and coupling terms) and CEM, respectively.

clamped–free boundary condition are used. This is also confirmed by an inspection of the matrix shown in Appendix B where the off-diagonal (coupling) terms are not small. Table 3 shows the results using shape functions with the clamped–free boundary conditions and with the coupling terms in the stiffness matrix. It is

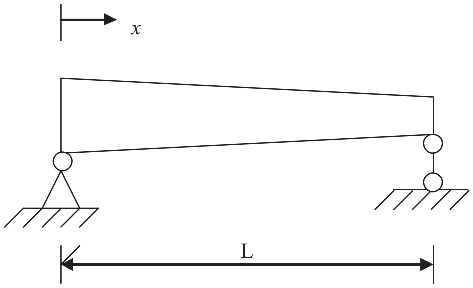

Fig. 2. A simply supported beam with varied depth.

Table 4
Comparison of natural frequencies (Hz) for Example 2

FEM	Original CEM	Modified CEM (with coupling term only)	Modified CEM (with shape functions only)	Modified CEM (with shape functions and coupling terms)
8.257	8.378	8.258	8.402	8.258
33.568	31.773	33.570	34.626	33.570
75.338	74.602	75.348	81.133	75.345
133.742	116.918	133.770	144.540	133.755

noted that the results are more close to the analytical solutions than those from the CEM when the above mentioned modifications are included.

3.2. Natural frequencies of a tapered beam

The deficiency of the original CEM is further illustrated with a non-uniform beam. Fig. 2 shows a tapered beam with linearly varied depth. The parameters of the beam are: Young's modulus $E = 200\,\text{Gpa}$, mass density $\rho = 7850\,\text{kg/m}^3$, length $L = 2\,\text{m}$, width $w = 0.02\,\text{m}$, the beam depth is expressed as

$$h(x) = \left(1 - 0.5\frac{x}{L}\right). \tag{5}$$

Again, the beam is modeled with a single beam element and 5c-dof is chosen. Table 4 shows the first four natural frequencies from the original CEM and those from the modified CEM. The results of CEM with both types of modifications are found much closer to those from finite element analysis than those from the original CEM.

4. Conclusions

The simulation studies above show that the original CEM is restricted to the case of clamped–clamped beam elements and is not applicable to members with non-uniform cross-sections unless the improvements suggested in the present discussion are provided.

Appendix A

Shape functions for different beam boundary conditions are shown in Table A1.

Table A1
Shape functions for different beam boundary conditions

Boundary condition	Mode shape	β_n
Free–free	$\cosh \alpha_n x + \cos \alpha_n x - \beta_n(\sinh \alpha_n x + \sin \alpha_n x)$	0.9825, 1.0008, 0.9999, 1.0, 0.9999 for $n = 1, \ldots, 5$. $\beta_n = 1.0$ for $n > 5$
Clamped–free	$\cosh \alpha_n x - \cos \alpha_n x - \beta_n(\sinh \alpha_n x - \sin \alpha_n x)$	0.7341, 1.0185, 0.9992, 1.0, 1.0 for $n = 1, \ldots, 5$. $\beta_n = 1.0$ for $n > 5$
Clamped–clamped	$\cosh \alpha_n x + \cos \alpha_n x - \beta_n(\sinh \alpha_n x + \sin \alpha_n x)$	0.9825, 1.0008, 0.9999, 1.0, 0.9999 for $n = 1, \ldots, 5$. $\beta_n = 1.0$ for $n > 5$
Pinned–pinned	$\sin(n\pi x/L)$	N/A

Appendix B

Stiffness matrix of a 5c-dof composite beam element with different boundary conditions are shown below.
Clamped–clamped beam element:

$$K_e = \frac{EI}{L^3}\begin{bmatrix} 12 & 6 & -12 & 6 & 0 & -1\times10^{-4} & -2\times10^{-4} & -1\times10^{-4} & -7\times10^{-4} \\ 6 & 4 & -6 & 2 & 0 & -1\times10^{-4} & -1\times10^{-4} & -1\times10^{-4} & -4\times10^{-4} \\ -12 & -6 & 12 & -6 & 0 & 1\times10^{-4} & 2\times10^{-4} & 1\times10^{-4} & 7\times10^{-4} \\ 12 & 2 & -6 & 4 & 0 & 0 & -1\times10^{-4} & 0 & -3\times10^{-4} \\ 0 & 0 & 0 & 0 & 1.035936\lambda_1^4 & 0 & 0 & 0 & 0 \\ -1\times10^{-4} & -1\times10^{-4} & 1\times10^{-4} & 0 & 0 & 0.998447\lambda_2^4 & 0 & 0 & 0 \\ -2\times10^{-4} & -1\times10^{-4} & 2\times10^{-4} & -1\times10^{-4} & 0 & 0 & 1.000067\lambda_3^4 & 0 & 0 \\ -1\times10^{-4} & -1\times10^{-4} & 1\times10^{-4} & 0 & 0 & 0 & 0 & 0.9999971\lambda_4^4 & 0 \\ -7\times10^{-4} & -4\times10^{-4} & 7\times10^{-4} & -3\times10^{-4} & 0 & 0 & 0 & 0 & 1.0\lambda_5^4 \end{bmatrix}.$$

Clamped–free beam element:

$$K_e = \frac{EI}{L^3}\begin{bmatrix} 12 & 6 & -12 & 6 & -7.482 & -33.380 & 71.293 & -53.977 & 72.823 \\ 6 & 4 & -6 & 2 & -6.494 & -7.129 & 19.701 & -15.993 & 22.274 \\ -12 & -6 & 12 & -6 & 7.482 & 33.380 & -71.293 & 53.977 & -72.823 \\ 12 & 2 & -6 & 4 & -0.988 & -26.296 & 51.592 & -37.985 & 50.549 \\ -7.482 & -6.494 & 7.482 & -0.988 & 1.0000\lambda_1^4 & 0 & 0 & 0 & 0 \\ -33.380 & -7.129 & 33.380 & -26.296 & 0 & 1.0004\lambda_2^4 & 0 & 0 & 0 \\ 71.293 & 19.701 & -71.293 & 51.592 & 0 & 0 & 1.0041\lambda_3^4 & 0 & 0 \\ -53.977 & -15.993 & 53.977 & -37.985 & 0 & 0 & 0 & 0.9545\lambda_4^4 & 0 \\ 72.823 & 22.274 & -72.823 & 50.549 & 0 & 0 & 0 & 0 & 0.9646\lambda_5^4 \end{bmatrix}.$$

References

[1] P. Zeng, Composite element method for vibration analysis of structures, part I: principle and C0 element (bar), *Journal of Sound and Vibration* 218 (4) (1998) 619–658.

[2] P. Zeng, Composite element method for vibration analysis of structures, part II: principle and C1 element (beam), *Journal of Sound and Vibration* 218 (4) (1998) 659–696.

[3] O.C. Zienkiewicz, *The Finite Element Method*, McGraw-Hill, London, 1997.

[4] D.J. Inman, *Engineering Vibration*, first ed., Prentice-Hall, Englewood Cliffs, NJ, 1994.